Inorg. Chem. **2004**, *43*, 3159–3163

Inorganic Chemistry
Article

Synthesis and Characterization of a New Three-Dimensional Lanthanide Carboxyphosphonate: $Ln_4(H_2O)_7[O_2C{-}C_5H_{10}N{-}CH_2{-}PO_3]_4(H_2O)_5$

Christian Serre,*,† Norbert Stock,‡ Thomas Bein,‡ and Gérard Férey†

*Institut Lavoisier, UMR CNRS 8637, Université de Versailles St-Quentin-en-Yvelines,
45 Avenue des Etats-Unis, 78035 Versailles Cedex, France, and Department of Chemistry,
Ludwig-Maximilians-University, Butenandtstrasse 5-13, Haus E, 81377 Munich, Germany*

Received November 25, 2003

The first open-framework lanthanide carboxyphosphonate has been obtained under hydrothermal conditions. The three-dimensional structure of MIL-84(Pr) (MIL = Material Institut Lavoisier) or $Pr_4(H_2O)_7[O_2C{-}C_5H_{10}N{-}CH_2{-}PO_3]_4(H_2O)_5$ has been solved from X-ray diffraction single-crystal data ($a = 23.481(1)$ Å, $b = 10.159(1)$ Å, $c = 23.006(1)$ Å, $\beta = 105.63(1)°$, $V = 5284.6(6)$ Å^3, space group *Cc* (No. 9)). Its framework is built up from chains of edged-sharing eight or nine-coordinated monocapped square antiprism polyhedra and carboxyphosphonate anions, creating a three-dimensional structure with small pores filled with water molecules. The thermal behavior of MIL-84(Pr) has been investigated using TGA and X-ray thermodiffractometry and indicates that MIL-84(Pr) is stable up to 523 K with a reversible hydration–dehydration process. The optical study of its yttrium analogue doped at 3.4% with europium (MIL-84(Y,Eu)) reveals a significant red-orange emission under UV radiation.

Introduction

The search for novel porous hybrid inorganic−organic materials is still of interest because of the wideness of their potential applications (shape-selective absorption, catalysis, molecular-based magnetism, hydrogen storage, ...).[1−8] The first synthetic routes were developed by Robl[1] and Clearfield[2] on the basis of the connection of inorganic moieties by functionalized organic molecules with complexing groups such as phosphonates, carboxylates, or sulfonates. Recently, several new design strategies have been set up and the number of characterized hybrid solids is exploding. This has led to some spectacular results such as the MOF solids reported by Yaghi and co-workers where a secondary building unit approach is used, leading to very large nanoporous materials with a controlled pore size.[9] Within the periodic table, d-block elements are usually preferred over f-block elements for the construction of hybrid solids, since the latter have high and variable coordination environments.[10] While the introduction of lanthanide centers within the skeleton may create unusual architectures, it may also give unique properties due to their f−f electronic transitions.[11] However, most of the lanthanide-based hybrid solids discovered up to now are coordination polymers in which the metallic moieties are either single polyhedra or isolated small clusters. Some 3D coordination polymers have been reported using dicarboxylates,[12−21] sulfonates,[22] and bipyridine.[23] This

---

* Author to whom correspondence should be addressed. Fax: (1) 39 25 43 58. Phone: (1) 39 25 43 05. E-mail: serre@chimie.uvsq.fr.

† Université de Versailles St-Quentin-en-Yvelines.

‡ Ludwig-Maximilians-University.

(1) Robl, C. *Mater. Res. Bull.* **1992**, *27*, 99.
(2) Clearfield, A. *Curr. Opin. Solid State Mater. Sci.* **1996**, *1*, 268−278.
(3) Feng, S.; Xu, R. *Acc. Chem. Res* **2001**, *34*, 239.
(4) Seo, J. S.; Whang, D.; Lee, H.; Jun, S. I.; Oh, J.; Jeon, Y. J.; Kim, K. *Nature* **2000**, *404*, 982.
(5) Yaghi, O. M.; O'Keeffe, M.; Ockwig, N. W.; Chae, H. K.; Eddaoudi, M.; Kim, J. *Nature* **2003**, *423*, 705−714.
(6) Férey, G. *Nat. Mater.* **2003**, *2*, 136−137.
(7) Rosi, N. L.; Eckert, J.; Eddaoudi, M.; Vodak, D. T.; Kim, J.; O'Keeffe, M.; Yaghi, O. M. *Science* **2003**, *300*, 1127−1129.
(8) Férey, G.; Latroche, M.; Serre, C.; Millange, F.; Loiseau, T.; Percheron-Guégan, A. *Chem. Commun.* **2003**, 2976.
(9) Eddaoudi, M.; Moler, D. B.; Li, H.; Chen, B.; Reineke, T.; O'Keefe, M.; Yaghi, O. M. *Acc. Chem. Res.* **2001**, *34*, 319.
(10) Kim, J. Y.; Norquist, A. J.; O'Hare, D. *Chem. Mater.* **2003**, *15*, 1970−1975.
(11) Antic-Fidancev, E.; Serpaggi, F.; Férey, G. *J. Alloys Compd.* **2002**, *340*, 88−94.
(12) Cao, R.; Sun, D.; Liang, Y.; Hong, M.; Tatsumi, K.; Shi, Q. *Inorg. Chem.* **2002**, *41*, 2087.
(13) Pan, L.; Huang, X.; Li, J.; Wu, Y.; Zheng, N. *Angew. Chem., Int. Ed.* **2002**, *39*, 527.
(14) Reineke, T. M.; Eddaoudi, M.; Fehr, M.; Kelley, D.; Yaghi, O. M. *J. Am. Chem. Soc.* **1999**, *121*, 1651.
(15) Wan, Y.; Jin, L.; Wang, K.; Zhang, L.; Zheng, X.; Lu, S. *New J. Chem.* **2002**, 1590.
(16) Wang, Z.; Jin, C.-M.; Shao, T.; Li, Y.-Z.; Zhang, K.-L.; Zhang, H.-T.; You, X.-Z. *Inorg. Chem. Commun.* **2002**, *5*, 642.
(17) Wu, L. P. *J. Coord. Chem.* **1996**, *37*, 361.

10.1021/ic035363p CCC: $27.50

leads to a drastic decrease in their performance and/or their thermal stability required for applicable properties. Our group recently reported a series of rare-earth solids built up from one- or two-dimensional inorganic subnetworks and aliphatic carbon chains such as diphosphonates[24] and di- and tricarboxylates.[25−31] In the field of carboxyphosphonates, most results are obtained using divalent cations.[32−35] However, one three-dimensional nonporous rare-earth carboxyphosphonate has been reported before.[36] This paper deals with the synthesis, the crystal structure, and the thermal behavior of the first microporous three-dimensional lanthanide carboxyphosphonate, $Pr_4(H_2O)_7((O_2C-C_5H_{10}N-CH_2-PO_3)_4)(H_2O)_5$ (MIL-84(Pr); MIL = Material Institut Lavoisier) and the optical properties of the isostructural Y compound doped with small amounts of Eu (MIL-84(Y,Eu)).

Experimental Section

Synthesis and Chemical Analysis. MIL-84(Pr) was hydrothermally synthesized (autogenous pressure for 5 days) at 483 K from a mixture of rare-earth nitrate $Pr(NO_3)_3{\cdot}5H_2O$ (Aldrich, 98%), the carboxyphosphonic acid $H_2O_3P-CH_2-NC_5H_{10}-CO_2H$, sodium hydroxide (NaOH) (Prolabo, 99%), and H_2O in the molar ratio 1:1:2:400. Concerning MIL-84(Y,Eu), the synthetic ratio was 1:1.5:2.5:400 with a Eu/(Eu + Y) ratio of 0.02. Reactants were introduced in this order and stirred for a few minutes before the resulting suspensions were introduced into a Teflon-lined steel autoclave. The final pH evolved from 4 to 3, which led to single crystals (Pr) or crystalline powders (Y, Eu) on which chemical analyses were performed. The reaction output is estimated at 75% on the basis of the rare-earth content.

The carboxyphosphonic acid $H_2O_3P-CH_2-NC_5H_{10}-COOH{\cdot}2H_2O$ was synthesized starting from piperidine-4-carboxylic acid using a Mannich-type reaction. In a typical experiment 0.05 mol (6.458 g) and 0.05 mol of crystalline phosphoric acid (4.1 g) are dissolved in a mixture of 5 mL of H_2O und 5 mL of concentrated HCl. The solution is heated to reflux, and 0.052 mol of an aqueous solution of formaldehyde (37%, 3.87 mL) is slowly added. After 2 h the reaction is stopped, and the mixture is slowly cooled to room temperature. The product is obtained as a microcrystalline powder.

Characterizations. The micrographs of single crystals of MIL-84(Pr) were realized on a JEOL JSM6500F field emission electron microscope.

The IR spectrum of MIL-84(Pr), obtained on a Bruker IFS 66v/S (KBr pellet prepared in a glovebox), clearly shows the presence of the vibrational bands characteristic of the −(O−C−O)− and −(O−P−O)− groups around 1550 and 1430 cm^{-1} and 1000 cm^{-1}, respectively, confirming the presence of the carboxyphosphonate within the solids.

The density measurement, performed on MIL-84(Pr) using a Micromeretics apparatus, Accupyc 1330, was 2.05(1) $g{\cdot}cm^{-3}$ (calcd 2.091 $g{\cdot}cm^{-3}$).

A TGA experiment, performed under a helium atmosphere on MIL-84(Pr) using a Setaram TG-DTA92 apparatus (heating rate 5 °C/min), has shown several weight losses in the 273−873 K range. The residual solid has been identified as praseodymium phosphate ($PrPO_4$). The first loss of 13.7% between 373 and 473 K corresponds to the departure of the free and bound water molecules, while the second loss of 27.5% observed around 773 K corresponds to the departure of organic moieties followed by their partial replacement by oxygen atoms to form the dense $PrPO_4$ at higher temperatures. These losses are in agreement with the theoretical values (13.4% and 28.7%, respectively).

X-ray thermodiffractometry, performed in the furnace of a Siemens D-5000 diffractometer in the $\theta-\theta$ mode, shows several steps in the decomposition for MIL-84(Pr).

Praseodymium and carbon contents were determined for MIL-84(Pr) at the CNRS Central Laboratory of Analysis of Vernaison (69, France); the Pr, P, N, and C contents are 32.6(3)%, 7.6(2)%, 3.2(2)%, and 20.3(7)%, which are on the whole in agreement with the theoretical values (34.4%, 7.58%, 3.36%, and 20.54%). Elemental analysis in a scanning electron microscope equipped with an EDX detector was performed to determine the semiquantitative yttrium-to-europium ratio in MIL-84(Y,Eu) using a JEOL 5800LV apparatus; five different analyses were realized, giving a Eu/(Eu + Y) ratio of 0.034(4).

The excitation of MIL-84(Y,Eu) was provided by a 450 W xenon lamp using an excitation wavelength of 384.8 nm, and the signal was recorded on an Edinburgh FL/FS 900 spectrometer system. The detector was a Si photodetector (OT900).

Finally, these analyses are on the whole in agreement with the results deduced from the structure determination of MIL-84(Pr) or $Pr_4(H_2O)_7((O_2C-C_5H_{10}N-CH_2-PO_3)_4)(H_2O)_5$.

Structure Determination. A rodlike single crystal of MIL-84-(Pr) suitable for data collection was glued onto a glass fiber. The structure determination by X-ray diffraction was performed on an Enraf-Nonius Kappa-CCD diffractometer equipped with a rotating anode (Mo Kα radiation, $\lambda = 0.71073$ Å) operating at 55 kV and 75 mA. The reflections were corrected for Lorentz and polarization effects and absorption. The cell of MIL-84(Pr) is monoclinic, space group *Cc* (No. 9). Details of the structure determination are given in Table 1.

The structure was solved using the SHELXTL package.[37] Praseodymium and most of the oxygen and carbon atoms were first located, while the remaining carbon atoms and the water molecules were found using difference Fourier maps. Hydrogen atoms of the organic groups were fixed using distance and angle constraints. The final reliability factors[37] converged to R1(F) = 0.0476 and

---

(18) Wu, L. P.; Munakata, M.; Kuroda-Sowa, T.; Maekawa, M.; Suenaga, Y. *Inorg. Chem. Acta* **1996**, *249*, 183.
(19) Wu, Y.; Zheng, N.; Yang, R.; Xu, H.; Ye, E. *J. Mol. Struct.* **2002**, *610*, 181.
(20) Xu, H.-T.; Zheng, N.-W.; Jin, X.-L.; Yang, R.-Y.; Li, Z.-Q. *J. Mol. Struct.* **2003**, *654*, 183.
(21) Paz, F. A. A.; Klinowsky, J. *Chem. Commun.* **2003**, 1484.
(22) Xiong, R.-G.; Zhang, J.; Chen, Z.-F.; You, X.-Z.; Che, C.-M.; Fun, H.-K. *J. Chem. Soc., Dalton Trans.* **2001**, 780.
(23) Long, D.-L.; Blake, A. J.; Champness, N. R.; Wilson, C.; Schröder, M. *J. Am. Chem. Soc.* **2001**, *123*, 3401.
(24) Serpaggi, F.; Férey, G. *J. Mater. Chem.* **1998**, *8*, 2749−2755.
(25) Serpaggi, F.; Férey, G. *J. Mater. Chem.* **1998**, *8*, 2737−2741.
(26) Serpaggi, F.; Férey, G. *Microporous Mesoporous Mater.* **1999**, *32*, 311−318.
(27) Serpaggi, F.; Férey, G. *J. Mol. Struct.* **2003**, *656*, 201−206.
(28) Serre, C.; Férey, G. *J. Mater. Chem.* **2002**, *12*, 3053.
(29) Serre, C.; Millange, F.; Marrot, J.; Férey, G. *Chem. Mater.* **2002**, *14*, 2409−2415.
(30) Serre, C.; Pellé, F.; Gardant, N.; Férey, G. *Chem. Mater.* **2004**, *16*, 2177.
(31) Serre, C.; Millange, F.; Thouvenot, C.; Gardant, N.; Pellé, F.; Férey, G. *J. Mater. Chem.*, in press.
(32) Stock, N. *Solid State Sci.* **2002**, *4*, 1089.
(33) Stock, N.; Bein, T. *Angew. Chem.*, in press.
(34) Stock, N.; Frey, S.; Stucky, G. D.; Cheetham, A. K. *J. Chem. Soc., Dalton Trans.* **2000**, 4292.
(35) Stock, N.; Stucky, G. D.; Cheetham, A. K. *Chem. Commun.* **2000**, 2277.
(36) Serpaggi, F.; Férey, G. *Inorg. Chem.* **1999**, *38*, 4741−4744.

(37) Sheldrick, G. M., 5.03 ed., 1997.

Table 1. Crystallographic Parameters of MIL-84(Pr)

empirical formula	$Pr_4P_4O_{32}N_4C_{28}H_{72}$
mol wt	1664
density ($g \cdot cm^{-3}$)	2.091
cryst syst	monoclinic
space group	*Cc* (No. 9)
a (Å)	23.481(1)
b (Å)	10.159(1)
c (Å)	23.006(1)
β (deg)	105.63(1)
V (Å^3)	5284.6(6)
Z	4
radiation λ_{Mo}	0.7103
temp (K)	293(2)
F(000)	3072
cryst size (μm)	60 × 20 × 20
θ range for data collection (deg)	3.29−27.39
limiting indices	$-10 < h < +10$, $-13 < k < +12$, $-29 < l < +28$
no. of reflns collected	16414
no. of independent reflns	5497 ($4599 > 2\sigma(I)$)
refinement method	goodness of fit based on F^2
no. of data/params/restraints	5497/314/2
GOF on F^2	1.127
extinction coefficient	0.00035(4)
largest diff peak and hole	0.701/−0.776
abs coeff (cm^{-1})	3.837
final R indices ($I > 2\sigma(I)$)	$R1(F) = 0.0476$, $wR2(F^2) = 0.0913$

Table 2. Selected Bond Lengths of MIL-84(Pr)

Pr(1)−O(1)	2.45(1)	Pr(1)−O(6)	2.38(1)
Pr(1)−O(7)	2.76(1)	Pr(1)−O(8)	2.53(1)
Pr(1)−O(11)	2.45(1)	Pr(1)−O(15)	2.40(1)
Pr(1)−O(22)	2.49(1)	Pr(1)−O(23)	2.56(1)
Pr(2)−O(5)	2.43(1)	Pr(2)−O(7)	2.39(1)
Pr(2)−O(10)	2.58(1)	Pr(2)−O(12)	2.66(1)
Pr(2)−O(14)	2.50(1)	Pr(2)−O(15)	2.78(1)
Pr(2)−O(16)	2.48(1)	Pr(2)−O(17)	2.55(1)
Pr(2)−O(18)	2.47(1)		
Pr(3)−O(1)	2.53(1)	Pr(3)−O(2)	2.61(1)
Pr(3)−O(3)	2.38(1)	Pr(3)−O(8)	2.71(1)
Pr(3)−O(9)	2.43(1)	Pr(3)−O(20)	2.37(1)
Pr(3)−O(24)	2.57(1)	Pr(3)−O(25)	2.44(1)
Pr(4)−O(2)	2.38(1)	Pr(4)−O(3)	2.66(1)
Pr(4)−O(4)	2.46(1)	Pr(4)−O(5)	2.56(1)
Pr(4)−O(10)	2.60(1)	Pr(4)−O(13)	2.34(1)
Pr(4)−O(21)	2.55(1)	Pr(4)−O(26)	2.60(1)
Pr(4)−O(27)	2.50(1)		
P(1)−O(1)	1.52(1)	P(1)−O(2)	1.56(1)
P(1)−O(14)	1.50(1)	P(1)−C(1)	1.85(1)
P(2)−O(3)	1.53(1)	P(2)−O(5)	1.58(1)
P(2)−O(6)	1.51(1)	P(2)−C(8)	1.80(1)
P(3)−O(7)	1.54(1)	P(3)−O(8)	1.55(1)
P(3)−O(9)	1.55(1)	P(3)−C(15)	1.86(1)
P(4)−O(4)	1.51(1)	P(4)−O(10)	1.53(1)
P(4)−O(15)	1.50(1)	P(4)−C(22)	1.83(1)
O(11)−C(21)	1.17(2)	O(12)−C(14)	1.27(2)
O(13)−C(28)	1.29(2)	O(16)−C(14)	1.24(2)
O(18)−C(28)	1.21(2)	O(19)−C(7)	1.34(2)
O(20)−C(21)	1.26(2)	O(22)−C(7)	1.25(2)
N(1)−C(1)	1.47(2)	N(1)−C(3)	1.45(2)
N(1)−C(5)	1.38(2)	N(2)−C(8)	1.47(2)
N(2)−C(10)	1.63(2)	N(2)−C(12)	1.57(2)
N(3)−C(15)	1.51(2)	N(3)−C(17)	1.47(2)
N(3)−C(19)	1.44(2)	N(4)−C(22)	1.50(2)
N(4)−C(25)	1.49(2)	N(4)−C(26)	1.49(2)
C(2)−C(4)	1.52(2)	C(2)−C(6)	1.55(2)
C(2)−C(7)	1.50(2)	C(3)−C(4)	1.54(2)
C(5)−C(6)	1.52(2)	C(9)−C(11)	1.49(2)
C(9)−C(13)	1.46(2)	C(9)−C(14)	1.59(2)
C(10)−C(11)	1.44(2)	C(12)−C(13)	1.51(2)
C(16)−C(18)	1.52(2)	C(16)−C(20)	1.56(2)
C(16)−C(21)	1.55(2)	C(17)−C(18)	1.48(2)
C(19)−C(20)	1.50(2)	C(23)−C(24)	1.53(2)
C(23)−C(27)	1.50(2)	C(23)−C(28)	1.54(2)
C(24)−C(25)	1.53(2)	C(26)−C(27)	1.58(2)

$wR2(F^2) = 0.0913$. Bond valence calculations confirm the oxidation state (+III) of praseodymium.[38] Finally, the formula deduced from the structure determination is $Pr_4(H_2O)_7((O_2C{-}C_5H_{10}N{-}CH_{2-}PO_3)_4)(H_2O)_5$. Atomic coordinates and full distances and angles are given in the Supporting Information.

Results and Discussion

Structure Description. MIL-84(Pr) exhibits a three-dimensional structure built up from PrO_8 and PrO_9 polyhedra and carboxyphosphonate ions. The PrO_8 and PrO_9 polyhedra exhibit the geometry of a regular or slightly distorted monocapped square antiprism, respectively. Its structure possesses a one-dimensional inorganic subnetwork, built up from chains of edge-sharing rare-earth polyhedra, interconnected via the organic acids and thus creating an open-framework structure (Figure 1). Despite the steric demand of the organic moieties, small channels are present along the *b* and *c* axes filled with noncoordinating water molecules (Figure 2).

Each rare-earth atom is surrounded by eight (Pr(1), Pr(2)) or nine (Pr(3), Pr(4)) oxygen atoms coming either from the organic moieties or from terminal water molecules (Figure 3). The way bound water molecules, carboxylate, and phosphonate moieties are grafted to the inorganic network differs for each rare-earth center. In fact, two different types of environments are present. If each lanthanide cation is related to three different phosphonate moieties, the first group of rare-earth ions (Pr(1), Pr(2)) is connected to two carboxylate groups while the second group (Pr(3), Pr(4)) exhibits one carboxylate connection. The noncentrosymmetry of MIL-84 is due to the nonequivalence of each rare-earth ion within each subgroup. In fact, Pr(1) and Pr(3) are eight-coordinated, while Pr(2) and Pr(4) are nine-coordinated. There exists also one monodendate carboxylate group linked to Pr(1), while a chelating carboxylate moiety shares one edge with Pr(2). The number of independent terminal water molecules within each group of lanthanide varies also from one (Pr(1), Pr(2)) to two (Pr(3)) and three (Pr(4)). Besides, the interatomic distances are well defined (Table 2): Pr−O distances are usually within the 2.34(1)−2.77(1) Å range, while the C−C, C−O, P−O, and P−C distances are within the 1.44(2)−1.59(2), 1.27(2)−1.31(2), 1.50(1)−1.58(1), and 1.80(2)−1.86(2) Å ranges, respectively.

In the field of rare-earth carboxyphosphonate or diphosphonate solids,[24,36] only pillared compounds have been reported so far, and MIL-84 is the first example of an open-framework lanthanide carboxyphosphonate.

Thermal Behavior. The thermal stability of MIL-84(Pr) has been studied using X-ray thermodiffractometry, performed in the furnace of a Siemens D-5000 diffractometer in the $\theta - \theta$ mode. It shows that MIL-84 is stable up to 250 °C. The water departure leads also to several structural changes between 60 and 200 °C. Above 200 °C, a continuous

---

(38) Brese, N. E.; O'Keeffe, M. *Acta Crystallogr.* **1991**, *B47*, 192.

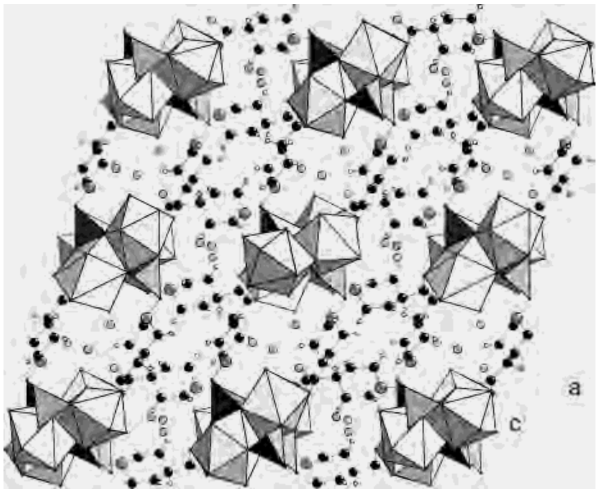

Figure 1. View of the structure of MIL-84(Pr) along the *b* axis. Praseodymium polyedra and phosphonate tetrahedra are in white and gray, while oxygen, carbon, nitrogen, and hydrogen atoms are represented in light gray, black, dark gray, and white, respectively.

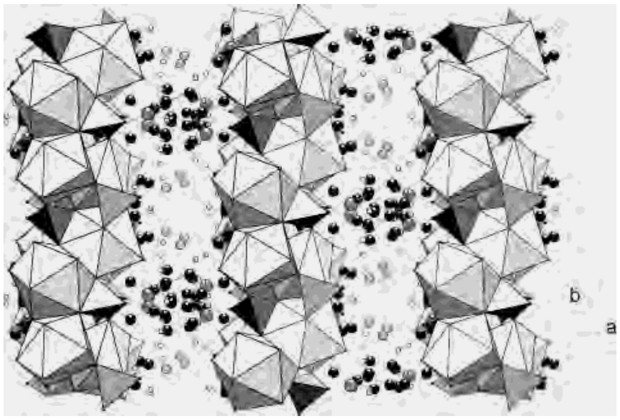

Figure 2. View of the structure of MIL-84(Pr) along the *c* axis. Praseodymium polyhedra and phosphonate tetrahedra are in white and gray, while oxygen, carbon, nitrogen, and hydrogen atoms are represented in light gray, black, dark gray, and white, respectively.

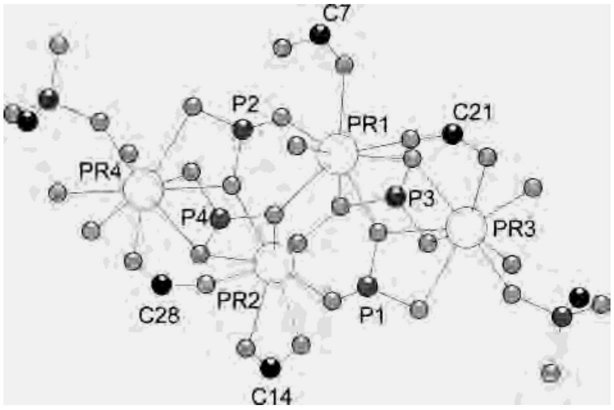

Figure 3. Schematic “balls and sticks” representation of the building unit of MIL-84(Pr). Praseodymium, phosphorus, oxygen, and carbon atome are represented in white, dark gray, light gray, and black, respectively.

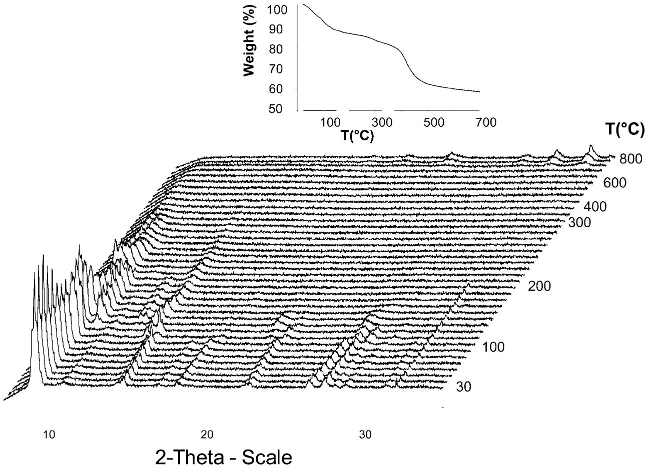

Figure 4. X-ray thermodiffractogram of MIL-84(Pr) under an air atmosphere. A TGA of MIL-84(Pr) performed under a helium atmosphere is represented in inset at the top of the figure.

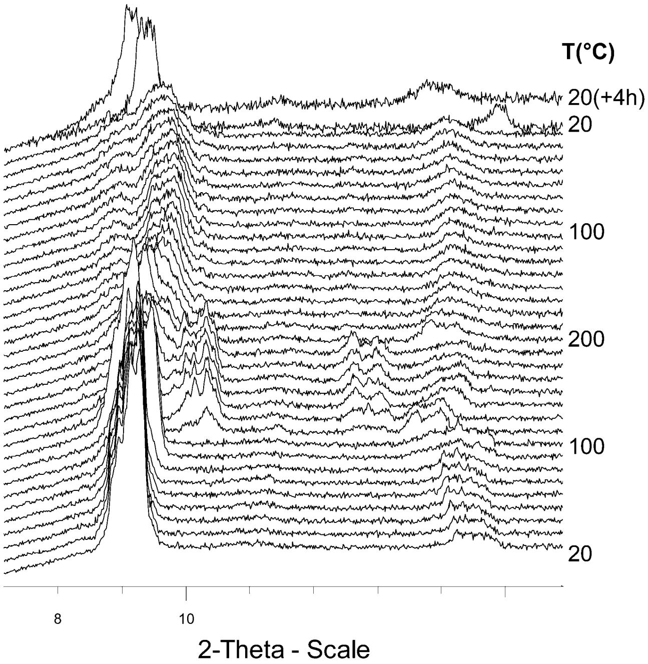

Figure 5. Study of the dehydration−hydration process of MIL-84(Pr) using X-ray thermodiffractometry under an air atmosphere. The last X-ray pattern was recorded 4 h after the sample was cooled back to 20 °C.

loss in crystallinity occurs followed at higher temperatures by formation of praseodymium phosphate, in agreement with TGA results (Figure 4). To study the reversibility of the water departures, a second X-ray thermodiffractometry experiment has been performed; it shows (Figure 5) that the water adsorption is fully reversible even if the free water uptake at room temperature seems relatively slow (see the smaller intensity of the first peak when back at 20 °C). A BET surface area measurement has been performed on MIL-84-(Pr) outgassed overnight at 150 °C and indicates that no accessible porosity exists for nitrogen ($S_{BET} = 11$ m^2/g).

Optical Properties. The yttrium analogue form of MIL-84 doped at 3.4% with europium (Eu/(Y + Eu) = 0.034)) has been prepared. TGA, quantitative analysis, and X-ray powder diffraction show that MIL-84(Pr) and MIL-84-(Y,Eu) are isostructural (see Figure 6). The optical properties of MIL-84(Y,Eu) were investigated at room temperature under UV excitation.

Five transitions at about 5750, 5900, 6100, 6500, and 7050 Å are observed in the emission spectra which are ascribed to the $^5D_0 \rightarrow {}^7F_J$ ($J = 0, 1, 2, 3, 4$) transitions of Eu^{3+} ions

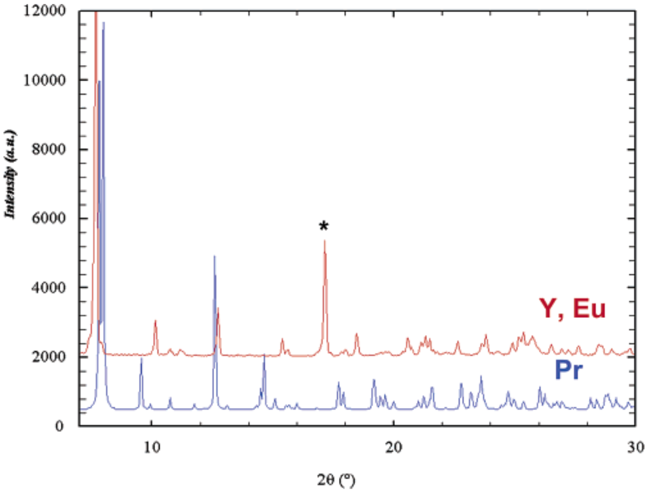

Figure 6. Comparison of the X-ray powder diffraction patterns of MIL-84(Y,Eu) and MIL-84(Pr) (calculated). Offsets have been applied for a better understanding. The asterisk indicates the main peak of the residual carboxyphosphonic acid.

(Figure 7). Several weak lines are recorded in the spectral range corresponding to the $^5D_0 \rightarrow {}^7F_0$ transition; this means that several optical sites are occupied by Eu^{3+} in that structure. As in the case of the previous yttrium–europium trimesate MIL-80,[31] the intensities of the $^5D_0 \rightarrow {}^7F_2$ and $^5D_0 \rightarrow {}^7F_1$ transitions are on the whole similar, indicating a weak asymmetry of the metallic europium sites. Further experiments including selective excitation will confirm the existence of several sites with different crystal field strengths.

In conclusion, MIL-84(Ln) is a new example of a luminescent three-dimensional rare-earth carboxyphosphonate characterized up to now with a one-dimensional inorganic subnetwork and a significant thermal stability. Other similar compounds are currently under study to enlarge the field of microporous hybrid phases based on rare-earth metals.

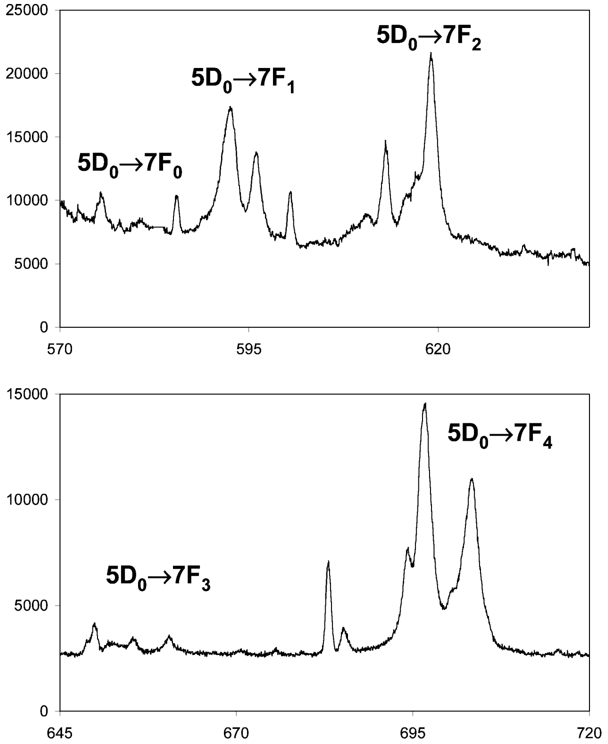

Figure 7. Fluorescence spectra of MIL-84(Y,Eu) at room temperature (excitation at 384.8 nm using a xenon lamp).

Supporting Information Available: X-ray crystallographic data in CIF format for MIL-84(Pr). This material is available free of charge via the Internet at http://pubs.acs.org. X-ray crystallographic data for MIL-84(Pr) have also been deposited at the Cambridge Crystallographic Data Centre (Deposition No. CCDC 224328).

IC035363P